Journal of Applied Polymer Science

Quinone Propionic Acid-Based Redox-Triggered Polymer Nanoparticles for Drug Delivery: Computational Analysis and *In Vitro* Evaluation

Jungeun Bae,[1] Manal A. Nael,[2] Lingzhou Jiang,[1] Patrick TaeJoon Hwang,[3] Fakhri Mahdi,[4] Ho-Wook Jun,[3] Wael M. Elshamy,[5] Yu-Dong Zhou,[4] S. Narasimha Murthy,[1] Robert J. Doerksen,[2,6] Seongbong Jo[1,6]

[1]Department of Pharmaceutics, School of Pharmacy, The University of Mississippi, University, Mississippi 38677
[2]Department of Medicinal Chemistry, School of Pharmacy, The University of Mississippi, University, Mississippi 38677
[3]Department of Biomedical Engineering, University of Alabama at Birmingham, 1825 University Boulevard, Birmingham, Alabama 35294
[4]Department of Pharmacognosy, School of Pharmacy, The University of Mississippi, University, Mississippi 38677
[5]Cancer Institute and Department of Biochemistry, University of Mississippi Medical Center, Jackson, Mississippi 39216
[6]Research Institute of Pharmaceutical Sciences, School of Pharmacy, The University of Mississippi, University, Mississippi 38677
Correspondence to: S. Jo (E-mail: seongjo@olemiss.edu)

ABSTRACT: Redox-responsive polymers with pendant quinone propionic acid groups as a redox trigger were optimized by computational modeling to prepare efficient redox-triggered polymer nanoparticles (NPs) for drug delivery. Lipophilicities at complete reduction of redox-responsive polymers (<5000 Da) constructed with adipic acid and glutaric acid were remarkably reduced to range from −6.29 to −0.39 compared with nonreduced state (18.87–32.46), suggesting substantial polymer solubility reversal in water. Based on this hypothesis, redox-responsive NPs were prepared from the synthesized polymers with paclitaxel as model cancer drug. The average size of paclitaxel-loaded NPs was 249.8 nm and their reconstitutions were stable over eight weeks. *In vitro* drug release profiles demonstrated the NPs to release >80% of paclitaxel over 24 h at a simulated redox-state compared with 26.5 to 41.2% release from the control. Cell viability studies revealed that the polymer was nontoxic and the NPs could release paclitaxel to suppress breast cancer cell growth. © 2014 Wiley Periodicals, Inc. J. Appl. Polym. Sci. **2014**, *131*, 40461.

KEYWORDS: stimuli-sensitive polymers; drug delivery systems; nanoparticles; nanowires and nanocrystals; applications; polyesters

Received 31 August 2013; accepted 16 January 2014
DOI: 10.1002/app.40461

INTRODUCTION

Cancer has been a major cause of mortality across the world.[1,2] Tremendous efforts have already been made to improve cancer therapy, including chemotherapy, in conjunction with nanotechnology as well as bioimaging.[3] Potent anticancer therapeutic agents are generally non-selective and thus affect normal cells, leading to severe side effects. Targeted drug delivery systems have been considered as a promising tool to minimize the toxicity by distributing the cytotoxic drugs favorably to tumor sites in the body. In particular, abnormal leaky tumor vasculatures and deficiency of lymphatic drainage in tumor enable nanotechnology-based targeted drug delivery to favorably accumulate cancer therapeutics in solid tumor while lessening their toxicity to normal tissues.[4] For selective drug release in tumor sites, stimuli-responsive polymer-based drug delivery systems have been extensively explored.[5] The bioresponsive delivery systems can undergo conformational or physiochemical property changes and release incorporated drugs in response to the signals stemming from tumor microenvironments such as acidic pH,[6,7] altered oxidation-reduction (redox),[8] over-expressed enzymes,[9] and hyperthermia.[10]

The alteration of the intracellular redox state is a noteworthy characteristic in cancer cells with consideration to the importance of redox homeostasis in maintaining cellular functions. The cellular redox systems employ endogenous enzymes, which tightly regulate intracellular redox via multiple cellular signaling pathways.[11] Thus, physiological or metabolic changes resulting from diseases affect cellular redox status via redox enzyme regulation.[12] In conjunction with the disease-related cellular redox changes, the redox gradient between intracellular and extracellular spaces has motivated the paradigm of redox-responsive biomaterials intended for intracellular drug delivery.[13]

DT-diaphorase (NAD(P)H : quinone oxidoreductase (NQO1), EC 1.6.99.2) is an obligate two-electron cytosolic reductase,

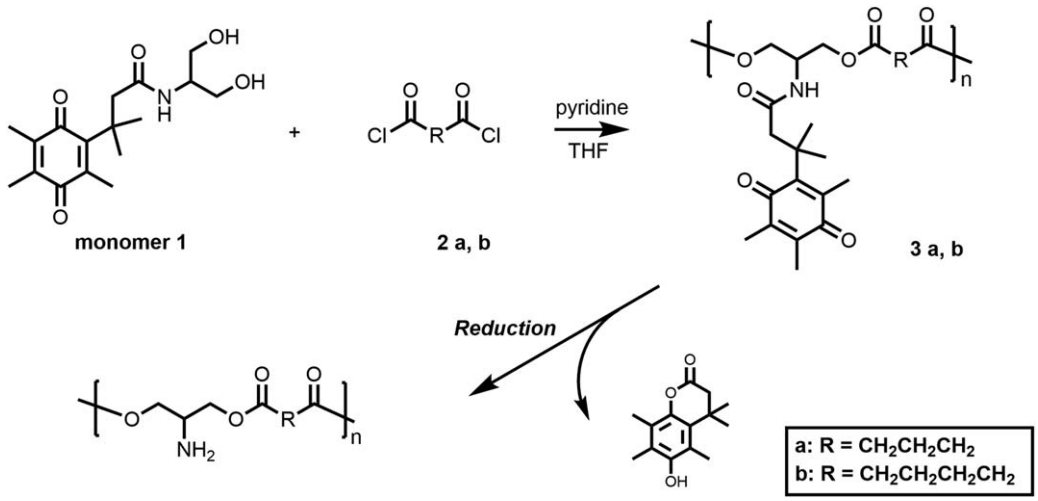

Scheme 1. Schematic synthetic reactions for redox-sensitive polymer with QPA and mechanism under reduction.

which reduces and detoxifies quinones and their derivatives as a part of an electrophilic and/or oxidative stress-induced cellular defense mechanism. DT-diaphorase is overexpressed in many cancerous tissues compared with surrounding normal tissues.[14] In the case of nonsmall-cell-lung tumors, DT-diaphorase activity determined using 2,6-dichlorophenolindophenol was found to be 123 nmol min^{-1} mg^{-1} compared with 6.4 nmol min^{-1} mg^{-1} in normal cells, a 20-fold increase. Since DT-diaphorase was known to activate quinone-bearing anticancer drugs, various quinone derivatives have been studied as a viable component of bioreductive cancer chemotherapeutics.[15] In addition, quinone-based bioreductive prodrugs, which release active cytotoxic drugs have been designed to selectively target cancer cells by overexpressed DT-diaphorase. Interestingly, trimethyl-locked quinone propionic acid (QPA) has been known to readily undergo intramolecular cyclization by DT-diaphorase-mediated two-electron reduction and release of a lactone. Because of this unique property of the QPA group, it has been extensively applied for cancer research as an efficient redox trigger.[16,17] Redox-triggered bioimaging probes consisting of QPA have been synthesized to liberate fluorescent indicators after DT-diaphorase-mediated activation.[18,19] Furthermore, QPA has been applied for the synthesis of bioreductive prodrugs based on aniline mustard[20] and oxindoles[21] for selective tumor targeting. QPA has also been coupled to dioleoyl phosphatidyl ethanolamine to prepare redox-responsive liposomes that can be triggered by a redox agent to release incorporated chemicals.[18]

In recent work, we have developed proof-of-concept redox-sensitive polymer nanoparticles (NPs) based on QPA chemistry and demonstrated redox-triggered drug release from the NPs.[22] Taking advantage of redox enzyme expression in tumor microenvironment would be an interesting strategy to target tumors because tumor tissues are hypoxic and usually show abnormal redox potential compared to normal tissues.[23] Here, we intended to optimize the molecular parameters associated with the QPA-based redox-sensitive NPs and evaluate their performance via both computational and experimental approaches. First, redox-responsive polyesters have been designed with a QPA-based diol monomer and dicarboxylic acids selected by theoretical calculations of polymer solubility represented with logP via computational modeling. Moreover, molecular dynamics (MD) of the redox-sensitive polymers and paclitaxel (PTX) was simulated to predict NP characteristics. Later, selected monomers were used for the synthesis of QPA-based redox-responsive polymers. The polymers were used for the preparation of PTX-loaded NPs. The NPs were evaluated for redox-triggered drug release under a simulated redox state. *In vitro* cytotoxicity of NPs was determined in human breast tumor T47D and MDA-MB-231 cells to determine cancer cell-mediated drug release.

EXPERIMENTAL

Materials

Methanesulfonic acid, 2,3,5-trimethyl hydroquinone, methyl β,β-dimethylacrylate, 2-amino-1,3-propanediol, adipoyl chloride, and glutaryl chloride were obtained from Alfa Aesar (Ward Hill, MA). Adipoyl chloride and glutaryl chloride were distilled under reduced pressure before the reaction. PTX was purchased from LC Laboratories® (Woburn, MA). Polyvinyl alcohol (PVA; $M_w = 30{,}000 - 70{,}000$) was obtained from Sigma-Aldrich (St. Louis, MO). All other chemicals purchased from Fisher Scientific (Pittsburg, PA) were used as received.

Computational Analysis

Polymer solubility was theoretically predicted by the calculation of logP with a group of polymer structures constructed from selected monomers. MD was simulated between a model drug, PTX, and the constructed redox-sensitive polymers to predict their interactions in NPs as well as NP stability for drug incorporation.

Polymer Construction. QPA-based redox-sensitive polyester structures were constructed by combinations between *N*-(1,3-dihydroxypropan-2-yl)−3-methyl-3-(2,4,5-trimethyl-3,6-dioxocyclohexa-1,4-dien-1-yl) (monomer 1 in Scheme 1, QPAMN)

and two dicarboxylic acids, glutaric acid, and adipic acid. According to the nature of the repeating units, the polymers were constructed head-to-tail in 3D using the polymer builder tool of molecular operating environment (MOE) software package (ver. 2011.10, Chemical Computing Group, Montreal, Canada). We considered the three possible degrees of reduction—nonreduced, partially reduced, and reduced—of QPA groups because of their potential effects on polymer solubility and drug release. Polymer chains of two molecular weights ~3000 and ~5000 Daltons were sketched.

Calculation of logP. The logP calculations used the weighted-method of ChemAxon suite (MarvinSketch 5.6.0.1, 2011, www.chemaxon.com), which is a combination of three algorithms, VG method (logP calculation according to various atom types),[24] KLOP method (group contribution approach),[25] and PHYSPROP (based on a logP database).[22] The logP calculated in this way is the arithmetic average of the three methods.

MD Simulation Between the Redox-Sensitive Polymers and PTX. PTX was constructed and energy minimized using MOE. We considered two polymer chains of five repeat units, $R = (CH_2)_4$ or $(CH_2)_3$ for this study. The conformational space of each polymer was searched using OMEGA version 2.4.6. We used the 94s variant of the Merck molecular force field (MMFF94s)[26] as the search force field. We considered an energy window of 10 kcal/mol to generate conformers and an RMSD cutoff of 0.5 Å to remove redundant ones. The lowest energy conformer of the polymer was used in the packing step. The Flory-Huggins interaction parameters χ were calculated using eq. (1).

$$\chi = \frac{V_r(\delta_1 - \delta_2)^2}{RT} \quad (1)$$

where R is the universal gas constant, V_r is the reference volume (100 cm^3/mol), T is the absolute temperature, and δ_1 and δ_2 are the Hildebrand solubility parameters for the drug and the polymer, respectively.[27] The Hildebrand solubility parameter is the square root of the cohesive energy density calculated by eq. (2).

$$\delta = \sqrt{CED} = \sqrt{\frac{(E_{vac} - E_{bulk})}{V}} \quad (2)$$

where V is the molar volume, E_{vac} and E_{bulk} are the potential energies in the vacuum state and in the bulk state.[28,29] The potential energy in vacuum state (E_{vac}) was obtained from Canonical (NVT) MD simulations without boundary conditions. A single chain of each polymer and a single drug molecule were individually minimized and then simulated for 3 ns at 310 K (Andersen thermostat) using a time step of 1 fs. The bonding and nonbonding interactions were parameterized with COMPASS force field.[30] For calculation of energy in bulk state (E_{bulk}), the polymers and the drug were simulated with the same settings but with application of periodic boundary conditions. The energy minimizations and MD simulations were carried out using Discover molecular simulation program version 2005.2 (Accelyrs Materials Studio 4.0, http://accelrys.com).

For simulating the NP on a minimal scale in relation to the actual size, the molecular packing program, packmol[31] was used to construct a sphere of 5 drug molecules with 10 Å diameters, after which 10 polymer chains were packed around the drug sphere. The diameter of the polymer-drug sphere was set to 25 Å. Water and NaCl were then added to construct a droplet of 50 Å. For the blank sphere, we packed only the 10 polymer chains with a diameter of 25 Å. The 3D structures of the packed spheres were minimized and parameterized using the all atom MMFF94× force field with no constraints. Canonical ensemble (NVT) MD simulations using NAMD[32] were performed with the following parameters: a checkpoint at 250 ps, sample time of 0.5 ps, NPA (Nosé-Poincaré-Anderson) Hamiltonian equations of motion, and time step of 0.0005 ps. We set the equilibration phase to 2 ns and the production phase to 50 ns. We simulated the spheres at 310 K. Solvent molecules were treated as rigid. Input files were prepared using MOE.

Synthesis of Polymers

The polymers theoretically predicted by computational modeling were synthesized in a similar way to the previous report.[22] Redox-sensitive monomer 1, QPAMN, was synthesized with *N*-hydroxysuccinimidyl QPA (NHS-QPA) and 2-amino-1,3-proanediol. Next, fresh distilled glutaryl chloride (242.7 mg, 1.44 mmol) was diluted ten times with dry THF and slowly added to the QPAMN solution (464.3 mg, 1.44 mmol) in pyridine at room temperature (Scheme 1). The reaction was further carried on at room temperature overnight. After being poured into an excess amount of ethanol and mixed for 6 h, it was extracted with deionized (DI) water and later with CH_2Cl_2. The collected organic phase was concentrated by a rotary evaporator and precipitated into cold diethyl ether to obtain the crude product, (3a, 470.8 mg). The adipic acid based polymer (3b, 571.4 mg) was synthesized with the same procedure shown above using 1.3 mL of pyridine monomer 1 (517.5 mg, 1.60 mmol) and dried adipoyl chloride (292.6 mg, 1.60 mmol). The structures of the synthesized polymers, 3a and 3b, were elucidated by ^{1}H-NMR spectra using a Bruker Avance 400 MHz spectrometer. The molecular weight and polydispersity index (PDI) of the synthesized polymers were determined with a Waters gel permeation chromatography (GPC) system (Waters, Milford, MA). GPC instrument is equipped with a binary pump (Waters 1525), a refractive index detector (Waters 2414), and a Styragel HR4E column (300 × 7.8 mm ID, 5 μm particle size). The measurement of the molecular weight was performed using HPLC grade THF as a mobile phase at a flow rate of 1.0 mL min^{-1} at 25°C. The molecular weight of the synthesized polymers was determined with the calibration curve obtained using polystyrene standards (600–50,000 Da). Under these conditions, retention times of 3a and 3b were 8.559 and 8.609 min, respectively. The number-average molecular weights (M_n) of the polymer 3a and 3b were found to be 6980 Da (PDI = 1.5) and 6477 Da (PDI = 1.7), respectively.

Polymer 3a: ^{1}H-NMR ($CDCl_3$): δ 6.30 (1H, s), 4.37 (1H, s), 4.12 (2H, s), 4.06 (2H, s), 2.83 (2H, s), 2.36 (4H, t), 2.11 (3H, s), 1.95 (8H, m), 1.39 (6H, s).

Preparation of Blank and PTX-Loaded NPs

The blank and PTX-loaded NPs were prepared by an emulsion method.[33] NPs-3a from polymer 3a and NPs-3b from polymer 3b were obtained through the same procedure. For preparation of PTX-loaded NPs, 40 mg of the synthesized redox-responsive

polymer and 4 mg of PTX were dissolved in 2 mL of CH_2Cl_2. This organic phase was slowly added to 18 mL of phosphate-buffered saline (PBS, pH 7.4) containing 0.7% of PVA mixing under magnetic stirring. The mixture was emulsified for 1 min in an ice bath by a probe sonicator (Qsonica, LCC. XL-2000, Newtown, CT). The emulsion was stirred overnight at room temperature to evaporate CH_2Cl_2. Aggregated NPs were filtered off with a 0.45 μm filter. The NPs were collected from the filtered solution by centrifugation (VWR^{TM} Galaxy 14D, 6,000 rpm, 15 min). The NPs were washed twice with PBS, 20 mL each time, and later with 20 mL of DI water to remove emulsifier. The produced suspension was lyophilized with the addition of 20 mg of mannitol to obtain fine powder of NPs. To prepare blank NPs, the above-mentioned procedures were employed except for leaving out PTX.

Characterization of Blank and PTX-Loaded NPs

The amount of PTX loaded in NPs was determined by dissolving a known weight (1.05 mg) of freeze-dried drug loaded NPs into 1 mL of acetonitrile and was analyzed via HPLC. The HPLC system is equipped with a Luna C18(2) chromatographic column (Phenomenex, 150 $\times$ 4.6 mm, 5 μm), a binary pump (Waters 1525), and an autosampler (Water 717). The mobile phase, a mixture of acetonitrile and water at 55/45% v/v, was used at a flow rate of 1 mL min^{-1} after injecting a 20 μL sample.[34] PTX was detected at a retention time of 4.9 min using a UV detector (Water 2487) at 227 nm. The concentration of released PTX was calculated using the calibration curve obtained from different concentrations of PTX standard solutions in 50% (v/v) aqueous acetonitrile. The percentage of PTX incorporated into NPs was calculated by dividing the amount of incorporated PTX with the initial PTX amount and multiplied by 100.

The size distribution and Z-average diameter of the NPs were determined by dynamic light scattering using a Zetasizer Nano ZS (Malvern Instruments, Worcestershire, UK). NP suspensions were diluted to a concentration of 1.25 mg NP in 1 mL of DI water. NP sizes were measured before freeze-drying and after reconstituting the NPs freeze-dried in the presence of mannitol to test the protective effect of mannitol during drying NPs.

For scanning electron microscope (SEM) analysis, NPs were reconstituted at a concentration of 1 mg mL^{-1} in DI water and homogeneously suspended by a 5 min sonication. A 50 μL aliquot of the reconstituted sample was mounted on an aluminum plate and dried. Then, the sample was sputter coated with gold and palladium. Quanta FEG 650 (FEI) at an accelerating voltage of 10 or 15 kv was used to image NPs.[35]

In Vitro Drug Release Studies

In vitro PTX release from the prepared NPs was conducted using $Na_2S_2O_4$ as a reducing agent. An amount of PTX-loaded NPs-3b containing 10 μg of PTX was suspended in 3 mL of PBS buffer (pH 7.4) containing 0.8*M* of sodium salicylic acid. The drug release was initiated by an addition of $Na_2S_2O_4$ to the NP suspension. A 200-fold molar excess of the reducing agent to QPA groups in the polymer was employed. Then, the mixture was incubated in a shaking water bath (100 rpm) at 37°C for 24 h. At designated times, a 150 μL aliquot of the NP sample was withdrawn from a vial after spinning down the NPs and an equal volume of fresh reducing medium was added and stirred into the NP solution. Samples were diluted with 150 μL of acetonitrile and the supernatant samples obtained with centrifugation (13,000 rpm, 3 min) were injected into the HPLC for analysis. The amounts of released PTX in the collected samples were determined by the same HPLC method as described in "Characterization of Blank and PTX-Loaded NP" except for external standard. The calibration curve was obtained from different concentrations of PTX standard solutions in 50% (v/v) aqueous acetonitrile. For the quantitative determination of lactone reduced from QPA groups, synthesized lactone was applied as external standard for HPLC analysis as previously reported.[22] The retention times of released lactone and PTX were 4.98 and 6.68 min, respectively, at 227 nm with an UV detector.

The drug release from NPs in cell media was also studied in Dulbecco's modified Eagle's medium (DMEM) supplemented with/without 5% fetal bovine serum (FBS). PTX-loaded NPs-3b (0.72 mg) were suspended into 1 mL of cell media incubating at 37°C. At designated time point over 48 h, 150 μL NP solution was withdrawn from the system and centrifuged at 10,000 rpm for 5 min to spin down NPs. Aliquots of 110 μL NP solution from supernatant media were mixed to the same amount of acetonitrile (110 μL) to remove protein precipitate. The remaining 40 μL solution including precipitated NPs was suspended with the same volume of fresh media and the suspension was added to the system to keep constant volume. After completing the collecting samples, the NP solution was mixed with the same volume of acetonitrile (1 mL) to measure the amount of PTX remaining in the NPs. To determine the amount of PTX, all collected samples were centrifuged to remove protein precipitate for the preparation of samples and HPLC method was used in the same manner as for the measurement in section "*In Vitro* Drug Release Studies."

Cell Viability Assay

Human breast tumor T47D and MDA-MB-231 cells obtained (ATCC, Manassas, VA) were grown in DMEM/F12 medium containing 2.5 m*M* L-glutamine (Mediatech), supplemented with FBS (10% v/v final concentration, Hyclone), penicillin G (sodium salt, 50 units mL^{-1}), and streptomycin sulfate (50 μg mL^{-1}) (BioWhittaker). Exponentially grown cells were plated at the density of 30,000 cells per well into 96-well plates in a volume of 100 μL culture media and incubated at 37°C in a humidified environment (95% air, 5% CO_2), as previously described.[36] PTX was dissolved in DMSO to obtain a 20 μM stock solution. PTX loaded NPs and blank NPs were prepared fresh as 100 μM stock solutions in PBS (pH 7.4). After compound treatment at the specified concentrations for 48 h, the cells were further incubated and cell viability was determined by the sulforhodamine B (SRB) method.[37] Optical density (OD) was measured at 490 nm with background absorption at 630 nm. Data were normalized to the untreated control and presented as "% of control," using the formula (3).

$$\text{Cell viability [\% of Control]} = (\text{OD}_{\text{treated}}/\text{OD}_{\text{control}}) \times 100 \quad (3)$$

Statistical Analysis

Experimental measurements were triplicated for each sample. The results are presented as mean $\pm$ standard deviation. The statistical analysis of experimental data used the student's t-

Table I. Calculated logP Values of QPA-Based Redox-Responsive Polymers at Different Degrees of Reduction

	MW = 5000			MW = 3000		
	Nonreduced	Partially reduced	Fully reduced	Nonreduced	Partially reduced	Fully reduced
Polymer **3a**	27.81	10.30	−6.29	18.87	7.21	−4.01
Polymer **3b**	32.46	16.27	−0.55	19.72	10.53	−0.39

Two polymer molecular weights, 3000 and 5000 Da, were chosen for comparison.

test and statistical significance was considered for *P*-values < 0.05.

RESULTS AND DISCUSSION

Computational Analysis and Polymer Synthesis

MD and molecular docking have been widely used in the process of drug development as means to predict and rationalize the design of drug delivery systems.[38] Theoretical calculation of logP provides rapid evaluation of lipophilicity and cellular penetration, which is widely used as a rational tool in the drug design process. Two polymers were constructed by combinations of previously synthesized QPAMN and dicarboxylic acids, glutaric acid and adipic acid. The main reason to select the two dicarboxylic acids was that NPs from the adipic acid-based redox-sensitive polymer have demonstrated redox-triggered content release by solubility reversal upon polymer reduction.[22] Two polymer molecular weights, 3000 and 5000 Daltons, were considered to test lipophilicities using ChemAxon. The logP calculated from the arithmetic average of the three ChemAxon logP methods including VG, KLOP and PHYSPROP showed the lower values in the reduced forms. As shown in Table I, fully reduced polymer with molecular weight of < 5000 Da showed the decrease of logP values of 3a and 3b from 27.81 to −6.29 and from 32.46 to −0.39, respectively. The logP values of polymer with MW < 3000 Da were similar and were lowered from 18.87 and 19.72 to −4.01 and −0.39 with the increase in reduction of polymers 3a and 3b, respectively. Reduction-dependent logP change in the polymers is probably due to the exposure of hydrophilic amine group upon removal of QPA. Especially, exposed primary amine groups would further lower polymer logP by protonation.

The polymers 3a and 3b, designed for redox-triggered NPs were synthesized as illustrated in Scheme 1.[22] The molar ratio of QPAMN to diacyl chlorides was 1.0 to achieve the highest possible polymer molecular weight which has reached 9000 Da previously. Polymer 3a synthesis yielded orange-yellow powders with a number-average molecular weight (M_n) of 6980 Da (PDI = 1.5). Polymer 3b was also synthesized and resulted in a M_n of 6477 Da (PDI = 1.7). Throughout this study, polymer synthesis has been reproducible to show a very narrow molecular weight variation with a standard deviation within 3% of polymer molecular weight. The ^{1}H-NMR spectra of the synthesized polymers were consistent with the structures previously reported. The chemical shift of -$\underline{CH_2}$—OH protons in QPAMN appearing at 3.32 ppm moved downfield to $\delta = 4.12$ and 4.06 ppm, indicating ester formation upon polymerization. Furthermore, characteristic methyl protons in QPAMN appearing at 1.41, 2.13, and 2.33 ppm were also found in the polymer NMR spectrum, which showed the incorporation of the intact QPA pendant group in the polymer backbone. The integration ratios of proton peaks on ^{1}H-NMR spectrum were consistent with the theoretical ratios of proton numbers in the polymer.

In this study, computational modeling has also been exploited to predict the formation of polymer NPs in water, preparing for effective experimental trials with less error. These follow the mechanism in scheme 1 for the delivery of encapsulated drug under reduction. Redox-responsive physicochemical property changes yielding polymers, which have higher lipophilicity in the nonreduced form allowing the compound with a good permeability and also to have increased water solubility after undergoing reduction. Based on the predicted changes in physicochemical properties, adipic acid, and glutaric acid based polymers would be ideal for the design of redox-sensitive NPs that are able to release incorporated drugs in a redox-triggered manner. NP assemblies were constructed (Figure 1) using MOE software and used for MD simulation performed on the two different polymer chains. We compared a packed NP with and without PTX to simulate loaded and blank NPs (Figure 1). The computed solubility parameters of PTX and both redox-sensitive polymers were summarized in Table II and applied to calculate the corresponding Flory-Huggins interaction parameters (χ). The χ values for PTX/polymer 3a and PTX/polymer 3b are 0.344 and 0.031, respectively. Both χ values are lower than the critical value of χ, 0.5, which indicate that PTX should be miscible with the selected polymers. The χ value of PTX/polymer 3b was lower than that for PTX/polymer 3a, which indicates higher PTX solubility for polymer 3b. Based on the χ values calculated by using δ parameters from the MD simulations (Table II), it was possible to predict that PTX and the selected redox sensitive polymers would be compatible.

Preparation of Redox-Responsive NPs

Redox-responsive NPs were prepared in the presence or absence of PTX from the synthesized polymers. An emulsion method using PVA was employed to obtain NPs with controlled particle sizes. Although particles smaller than 500 nm can be passively accumulated in tumor by the enhanced permeability and retention effect, NPs with particle sizes are <200 nm are generally considered as ideal for targeted drug delivery.[39] Emulsifying hydrophobic polymers and subsequent solvent evaporation have frequently yielded NPs suitable for tumor-targeted drug delivery.[40] The mean size of NPs-3a was determined to be 246.0 nm (PDI = 0.12) and 238.8 nm (PDI = 0.15), for the blank NPs and PTX-loaded NPs, respectively, as summarized in Table III.

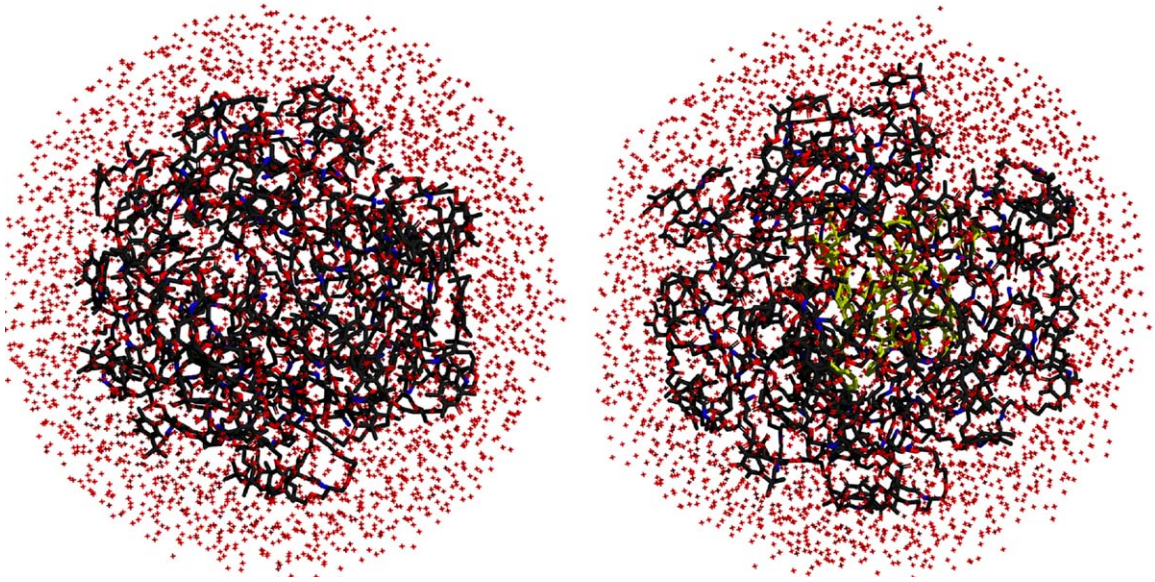

Figure 1. Blank (left) and PTX-loaded (right) NPs (constructed using packmol) after MD simulations using MOE software package. Gray = redox-sensitive polymer; yellow = PTX; red = water. [Color figure can be viewed in the online issue, which is available at wileyonlinelibrary.com.]

It was found that the use of surfactants for the preparation of redox-responsive NPs affected NP size. Tween 80 and Pluronic F68 indeed resulted in particle sizes ranging from 400 to 830 nm (data not shown). The nonionic stabilizers might differently affect the stability of the oil-in-water emulsions of the redox-responsive polymers. Droplet sizes of the emulsions could be an important factor for the size of final hardened polymer NPs. The sizes of our redox-responsive NPs were comparable to the particle sizes obtained with poly(D,L-lactide-*co*-glycolid) (PLGA).[41] The size of PLGA (MW = 75,000–120.000) NPs prepared with Pluronic F68 was 461 ± 10 nm, which was larger than the 284 ± 6 nm obtained with PVA.[41] This result indicated that PVA in CH_2Cl_2 could decrease interfacial tension more than Pluronic F68 did and, thus, lead to smaller particles size. The increase in size of obtained NPs was observed due to the aggregation of NPs when using Tween 80 and similar observations were also reported on the formation of poly(D,L-lactic acid) NPs emulsified with Tween 80.[41]

PTX loading into NPs-3a was determined to be 45% (w/w) as summarized in Table III. However, NPs-3b resulted in an enhanced drug loading of 77% (w/w). It looked as though an additional carbon in the polymer repeating unit in polymer 3b might be attributed to the difference in drug loading in two kinds of NPs. As previously observed, drug loading into polymer particles is closely related to drug solubility in the polymer. It is speculated that polymer 3b may have greater miscibility with PTX than polymer 3a because of greater hydrophobicity as predicted by theoretical logP calculations (Table I). In addition, Flory-Huggins' integration parameters (Table II) calculated from MD simulation are consistent with our observation of PTX loading, in which the stronger interaction between drug and polymer resulted in enhanced drug loading efficiency.

Aggregation of hydrophobic NPs during freeze drying has commonly been observed.[42] Carbohydrate stabilizers such as sucrose, lactose, glucose, sorbitol, and mannitol have been routinely employed to prevent the product from undergoing the stress that could destabilize colloidal suspension, which is generated during the freeze drying process.[43] For the freeze-drying of redox-sensitive polymer NPs prepared from QPA-based polymer, mannitol was added to minimize particle aggregation and improve the handling properties of the dried NPs. It should be noted that mannitol has been widely used as a cryoprotectant in the formulations of biotechnology products which are currently in the market.[44] It has also been known that mannitol tends to crystallize during freeze-drying process resulting in powdery and dry products, which usually improves handling property.[45] The protective effect of mannitol during freeze drying was examined by particle size measurements before and after NP drying. The size of redox-responsive NPs-3b before drying was determined to be 220.60 ± 21.56 nm (PDI = 0.16 ± 0.07). NP size slightly increased to 269.83 ± 21.56 nm (PDI = 0.24 ± 0.05) after reconstitution of the dried NPs into water (summarized in Table III). This slight particle size increase may be due to hydration of NPs. The redox-responsive polymer NPs seemed to be aggregated by interparticular hydrophobic interactions during freeze drying without mannitol.[46]

Table II. Solubility Parameters of PTX, Polymer 3a and Polymer 3b, and Flory-Huggins Interaction Parameters Computated using the Solubility Parameters

	Solubility parameters (δ; $(J/cm^3)^{1/2}$	Flory-Huggins interaction parameter (χ) for PTX and redox-sensitive polymer pairs
PTX	21.83	
Polymer 3a	18.91	0.344
Polymer 3b	20.95	0.0312

Table III. Mean Sizes of Prepared Redox-Responsive Polymer NPs and Drug Loading Efficiency into the NPs

NPs	Size (nm)		Drug loading efficiency (w/w)
	Mannitol-free	Drying with mannitol	
Blank NPs-3a	246.03 ± 42.58	322.07 ± 28.59	
PTX loded NPs-3a	238.8 ± 20.49	257.67 ± 43.89	45%
Blank NPs-3b	220.60 ± 21.56	269.83 ± 26.57	
PTX loded NPs-3b	256.47 ± 9.55	293.17 ± 13.21	77%

Mannitol was used to stabilize the particles during freeze-drying. PTX was used as a model drug.

It appears that NP aggregation was prevented by the presence of mannitol, which can hold water and fill spaces between NPs during the drying process. Drug loading did not noticeably diminish the protective role of mannitol to hinder particle aggregation. In the case of PTX-loaded NPs-3b, particle size was marginally increased from 256.47 ± 9.55 nm (PDI = 0.08 ± 0.03) to 293.17 ± 13.21 (PDI = 0.17 ± 0.06) for wet NPs before drying and reconstituted particles after freeze-drying, respectively, in the presence of mannitol (Table III). In addition, lyophilized NPs have maintained their stability over an eight week period (summarized in Figure 2). Reconstituted PTX-loaded NPs-3b have shown a modest particle size increase from 293.2 to 346.4 nm over an eight week incubation at 37°C (Figure 2). Interestingly, a noticeable change in particle size modification was observed with blank NPs, wherein the size of NPs increased from 269.8 to 558.5 nm in 4 weeks. The particle size further increased to 682.8 nm in another 4 weeks. The hydrophobic drug might have contributed to an improved stability of PTX-loaded NPs.

Other NPs prepared from gelatin, poly(D,L lactide-glycolide) and lipids have also demonstrated a similar mannitol-mediated protective effect with no significant particle size alteration after freeze drying.[47] In addition, as shown in Figure 3, mannitol was well integrated with the redox-responsive NPs-3b. The morphologies of NPs with or without PTX loading after drying in the presence of mannitol were different from that of freeze-dried mannitol as confirmed by SEM images. SEM images of dried mannitol revealed spherical particles with relatively uniformed size as well as rounded morphology [Figure 3(C)]. However, the microscopic images of dry NPs [Figure 3(A,B)] showed that mannitol has been integrated well with polymer NPs by showing chunks rather than segregated mannitol spheres. Mannitol integrated with the NPs might be distributed between particles as a space filler or as a coat on their surface, which prevents interparticular hydrophobic interactions between NPs.

In Vitro PTX Release

PTX release from the redox-responsive NPs was studied under a redox state simulated with a chemical reducing agent, sodium dithionite. Sodium dithionite has been frequently adopted in physiology experiments as a means to lower solutions' redox potential ($E = -0.66$ V at pH 7 at 0.35 nM[48]) and to mimic a reductive environment. Figure 4(A) shows that QPA-based redox-responsive NPs were able to release incorporated drug upon pendant QPA group reduction. Under a redox state simulated with sodium dithionite, the amounts of released PTX were significantly greater than PTX release in PBS [$P < 0.05$ for NPs-3a and NPs-3b at 15 min, $P < 0.01$ at 3 h, in Figure 4(A)]. Cumulative percentage of PTX released from two different NPs was more than 80% after a 24 h incubation under the redox state. However, only 41.2 and 26.5% of incorporated PTX were released from the NPs in the absence of the reducing agent. PTX release in the absence of sodium dithionite followed the release kinetics shown other references.[49,50] It was interesting to note that the NP from adipic acid-based redox-responsive polymer 3b showed PTX release comparable to that from NPs-3a, which was similar to the result previously obtained.[22] Lactone released from reduced QPA was consistent with PTX release indicating PTX release was mediated by lactone release. As previously discovered,[22] facilitated PTX release under the redox state can be attributed to QPA reduction which deprotects amine groups in the polymer backbone. Free amine groups exposed upon intramolecular cyclization of QPA could increase polymer solubility upon protonation at pH 7.4, which might result in NP swelling.[22] Theoretical calculations of hydrophobicity reduction upon polymer reduction, from 27.81 to −6.29 and from 32.46 to −0.55 for polymers 3a and 3b, respectively (Table I), also led to the prediction of polymer solubility increasing upon polymer reduction. In addition, exposed amine groups might contribute to the hydrolysis of the polyester backbone in a base-catalyzed manner.[51] As expected, NPs in the control release medium containing no reducing agent did not release quinone lactone at all [Figure 4(B)]. It is worthwhile to mention that NPs-3b showed lower initial PTX release than NPs-3a. The difference in burst PTX release from the NPs can be attributed to the polymer solubility difference. As previous

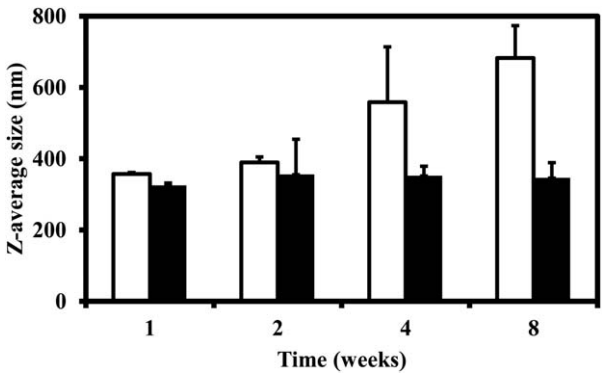

Figure 2. Size distribution of blank NPs-3b (□) and PTX-loaded NPs-3b (■) suspended in DI water and incubated at 37°C over eight weeks. Data shown as mean ± SD ($n = 3$).

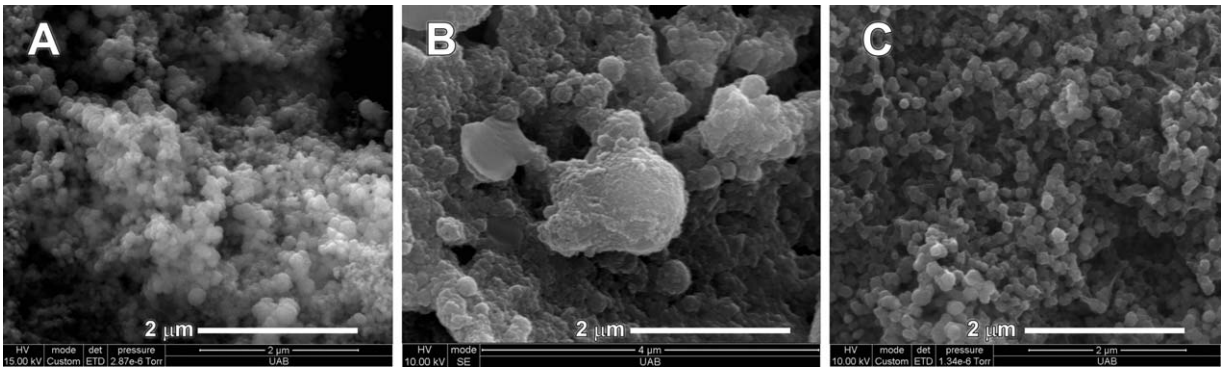

Figure 3. Scanning electron microscopy images of freezing dried NPs prepared with mannitol (A) PTX-loaded NPs-3b, (B) Blank NPs-3b, and (C) Freeze-dried mannitol (Scale bar = 2 μm).

theoretical calculations of polymer property predicted, polymer 3a is less hydrophobic than polymer 3b, which has one more carbon in polymer repeating unit. Predicted logP values (Table I) for nonreduced polymer 3a and 3b were 27.81 and 32.46, respectively, at a molecular weight of 5000 Da. It seemed that more hydrophobic polymer NPs-3b demonstrates the lower initial burst. Considering theoretical polymer property prediction and experimental drug release under a simulated redox state, NPs-3b would be more suitable for drug delivery applications, with a low burst drug release but maximized content release upon polymer reduction. However, drug release from the NPs by cancer cell-overexpressing redox enzymes should be further tested and confirmed before the implementation of the novel redox-responsive polymer NPs for tumor-targeted drug delivery.

In Vitro Cytotoxicity

Concentration-dependent cell cytotoxicity studies were performed to determine the effects of PTX–loaded redox-responsive NPs on the proliferation/viability of human breast tumor T47D and MDA-MB-231 cells. PTX-loaded and blank NPs-3a were used as positive and negative controls for the study, respectively. At the lower concentration range (0.01 μM or less), almost no cytotoxicity for both cell lines could be detected as shown in Figure 5. When the concentration was at 1 μM, the cell viability of T47D cell line with the incubation of PTX and PTX loaded NPs were 69 and 73%, respectively, while the result of cytotoxicity with blank NPs showed its less toxicity as 91% of cell viability in Figure 5(A). The cell experiment for MDA-MB-231 cell line in Figure 5(B) also showed similar cell viability, in which 48, 50, and 97% of cell viability were observed for plain drug, PTX loaded NPs, and blank NPs, respectively. PTX loaded NPs inhibited cell proliferation and viability to the comparable extent as that observed in the presence of PTX. The particle itself did not affect cell proliferation/viability at all concentrations tested indicating that all incorporated PTX has been released from NPs to limit cell growth.

Aside from *in vitro* cellular study, *in vitro* drug release from the NPs was examined to confirm culture cancer cell-mediated drug release from NPs using serum-free cell culture media and culture media supplemented with 5% FBS presented in Figure 6. The amounts of drug released from the NPs over 48 h ranged from 12.58 to 15.71% and from 10.89 to 14.66% in serum free DMEM and in DMEM with 5% FBS, respectively. In addition, the analysis of remaining NPs showed considerable amounts of PTX left in the NPs, indicating that FBS might contribute to drug release in part but not all. The amounts of drug found in the NPs were 86.05 and 53.67% in serum free DMEM and DMEM with 5% FBS, respectively. The reason for less drug retention in the presence of FBS might be the enzymes in FBS. It

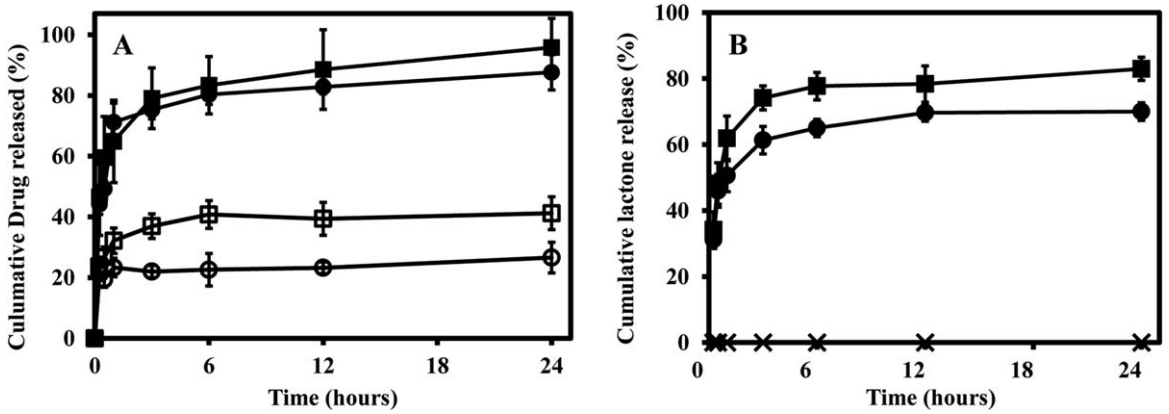

Figure 4. (A) *In vitro* redox-responsive release of PTX and (B) release of lactone from reduced QPA when incubated in the reductive media including $Na_2S_2O_4$ (• and ■) and at control media (○, □, and x) at 37°C from NPs-3a (• and ○) and from NPs-3b (■ and □). The results represent the mean ± SD ($n = 3$).

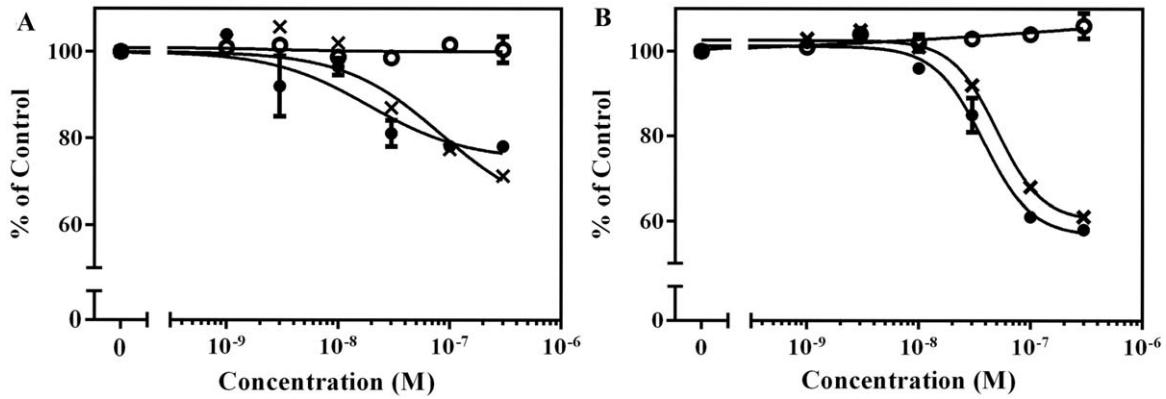

Figure 5. Effects of PTX-loaded NPs on human breast tumor cell proliferation/viability determined by SRB method: (A) T47D cells. (B) MDA-MB-231 cells. Exponentially grown T47D and MDA-MB-231 cells were exposed to the different concentration of PTX-loaded NPs (•), blank NPs (○), and PTX (×) for 48 h under normoxic condition (95% air : 5% CO_2). The percentage of viable cells was normalized to values obtained from untreated control under normoxia conditions, and presented as "% of Control." Data shown are average ± standard deviation ($n = 3$).

has been known that FBS contains a mixture of enzymes including esterases and proteases, which are able to degrade polyester backbone in the QPA-based redox-responsive polymer. Proteins in FBS, 23 g L^{-1} of albumin and 38 g L^{-1} of total protein, may also be able to affect polymer degradation, NP stability or PTX protein binding.[52] Indeed, PTX was reported to significantly bind to protein in cell culture media, which was PTX concentration dependent. PTX was known to result in 78.6 ± 2.7% protein binding at a concentration of 0.5 μg mL^{-1} in cell culture medium with 9% FBS and PTX binding to proteins decreased to 20.2 ± 1.4% as concentration of PTX increased to 15 μg mL^{-1}. The PTX protein binding might overestimate PTX release in FBS containing DMEM. However, taking cell cytotoxicity results and *in vitro* drug release in culture media together, cultured cancer cells could release PTX from the redox-responsive NPs.

CONCLUSIONS

Redox-responsive QPA-based polymers were analyzed with the aid of computational calculations and were used for the preparation of NPs that could release incorporated PTX under a redox state simulated with a redox agent. The NPs could be protected by mannitol during freeze drying process and NP stability has been maintained for a period of eight weeks. Prepared redox-responsive NPs were able to release 80% of incorporated PTX in a redox-triggered manner within 24 h. Cytotoxicity assay using cultured human breast tumor cell lines demonstrated that cancer cells could release incorporated drug from the NPs. These redox-sensitive NPs may be useful as delivery platforms for cytotoxic cancer drugs.

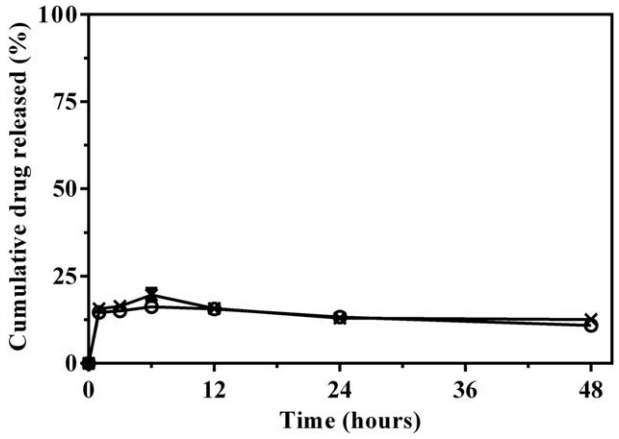

Figure 6. *In vitro* PTX release from NPs-3b in different cell culture media: serum-free cell culture media (○) and the media supplemented with 5% FBS (×). Data shown as mean ± SD ($n = 3$).

ACKNOWLEDGMENTS

The authors acknowledge that funding for this work came from Department of Defense W81XWH-10-1-0414 and National Science Foundation EPS-0903787 (S.J.). They also acknowledge the HRSA grant off which the Malvern Zetasizer was purchased. This work was also supported in part by the National Institutes of Health National Cancer Institute (grant CA98787; Y.-D. Z.). Jungeun Bae took a responsibility for the acquisition of the data, participated in polymer synthesis, analysis and the interpretation of the results. She also wrote the manuscript. Manal A. Nael and Dr. Robert J. Doerksen contributed to research design and were in charge of the computational analysis in this article. Lingzhou Jiang, Patrick TaeJoon Hwang and Dr. Ho-Wook Jun performed SEM experiment and data interpretation. Drs. Fakhri Mahdi and Yu-Dong Zhou were responsible for cell culture-based experiment. Drs. Wael M. Elshamy and S. Narasimha Murthy were involved in the analysis and interpretation of the data. Dr. Seongbong Jo supervised the research and manuscript preparation. All the authors partook in writing the article and have also consented to submit this article.

REFERENCES

1. Center, M. M.; Jemal, A.; Lortet-Tieulent, J.; Ward, E.; Ferlay, J.; Brawley, O.; Bray, F. *Eur. Urol.* **2012**, *61*, 1079.
2. Garcia, K.; Crimmins, E. M. In Applied Demography and Public Health; Hoque, N.; McGehee, M. A.; Bradshaw, B. S., Eds.; Springer: Netherlands, **2013**; Vol. 3, Chapter 9, pp 125–154.
3. Melancon, M. P.; Stafford, R. J.; Li, C. *J. Controlled Release* **2012**, *164*, 177.

4. Sailor, M. J.; Park, J.-H. *Adv. Mater.* **2012**, *24*, 3779.
5. Fleige, E.; Quadir, M. A.; Haag, R. *Adv. Drug. Delivery. Rev.* **2012**, *64*, 866.
6. Garripelli, V. K.; Namgung, R.; Kim, W. J.; Jo, S. *J. Biomater. Sci. Polym. Ed.* **2012**, *23*, 1505.
7. Kim, J. K.; Garripelli, V. K.; Jeong, U. H.; Park, J. S.; Repka, M. A.; Jo, S. *Int. J. Pharm.* **2010**, *401*, 79.
8. McCarley, R. L. *Annu. Rev. anal. Chem.* **2012**, *5*, 391.
9. Ku, T.-H.; Chien, M.-P.; Thompson, M. P.; Sinkovits, R. S.; Olson, N. H.; Baker, T. S.; Gianneschi, N. C. *J. Am. Chem. Soc.* **2011**, *133*, 8392.
10. Grüll, H. *J. Controlled Release* **2012**, *161*, 317.
11. Valko, M.; Leibfritz, D.; Moncol, J.; Cronin, M. T.; Mazur, M.; Telser, J. *Int. J .Biochem. Cell Biol.* **2007**, *39*, 44.
12. Trachootham, D.; Lu, W.; Ogasawara, M. A.; Nilsa, R. D.; Huang, P. *Antioxid. Redox. Signal.* **2008**, *10*, 1343.
13. Son, S.; Namgung, R.; Kim, J.; Singha, K.; Kim, W. J. *Acc. Chem. Res.* **2011**, *45*, 1100.
14. Smitskamp-Wilms, E.; Giaccone, G.; Pinedo, H.; van der Laan, B.; Peters, G. *Br. J. Cancer* **1995**, *72*, 917.
15. Ross, D.; Siegel, D.; Beall, H.; Prakash, A.; Mulcahy, R. T.; Gibson, N. W. *Cancer Metastasis Rev.* **1993**, *12*, 83.
16. Siegel, D.; Franklin, W. A.; Ross, D. *Clin Cancer Res.* **1998**, *4*, 2065.
17. Jamieson, D.; Wilson, K.; Pridgeon, S.; Margetts, J. P.; Edmondson, R. J.; Leung, H. Y.; Knox, R.; Boddy, A. V. *Clin. Cancer Res.* **2007**, *13*, 1584.
18. Ong, W.; Yang, Y.; Cruciano, A. C.; McCarley, R. L. *J. Am. Chem. Soc.* **2008**, *130*, 14739.
19. Silvers, W. C.; Prasai, B.; Burk, D. H.; Brown, M. L.; McCarley, R. L. *J. Am. Chem. Soc.* **2012**, *135*, 309.
20. Volpato, M.; Abou-Zeid, N.; Tanner, R. W.; Glassbrook, L. T.; Taylor, J.; Stratford, I.; Loadman, P. M.; Jaffar, M.; Phillips, R. M. *Mol. Cancer Ther.* **2007**, *6*, 3122.
21. Maskell, L.; Blanche, E. A.; Colucci, M. A.; Whatmore, J. L.; Moody, C. J. *Bioorg. Med. Chem. Lett.* **2007**, *17*, 1575.
22. Cho, H.; Bae, J.; Garripelli, V. K.; Anderson, J. M.; Jun, H.-W.; Jo, S. *Chem. Commun.* **2012**, *48*, 6043.
23. Brown, J. M. *Mol. Med. Today.* **2000**, *6*, 157.
24. Viswanadhan, V. N.; Ghose, A. K.; Revankar, G. R.; Robins, R. K. *J. Chem. Inform. Comput. Sci.* **1989**, *29*, 163.
25. Klopman, G.; Li, J.-Y.; Wang, S.; Dimayuga, M. *J. Chem. Inform. Comput. Sci.* **1994**, *34*, 752.
26. Halgren, T. A. *J. Comput. Chem.* **1999**, *20*, 720.
27. Miller-Chou, B. A.; Koenig, J. L. *Prog. Polym. Sci.* **2003**, *28*, 1223.
28. Belmares, M.; Blanco, M.; Goddard, W. A.; Ross, R. B.; Caldwell, G.; Chou, S. H.; Pham, J.; Olofson, P. M.; Thomas, C. *J. Comput. Chem.* **2004**, *25*, 1814.
29. Patel, S.; Lavasanifar, A.; Choi, P. *Biomacromolecules* **2008**, *9*, 3014.
30. Sun, H. *J. Phys. Chem. B.* **1998**, *102*, 7338.
31. Martinez, L.; Andrade, R.; Birgin, E. G.; Martinez, J. M. *J. Comput. Chem.* **2009**, *30*, 2157.
32. Phillips, J. C.; Braun, R.; Wang, W.; Gumbart, J.; Tajkhorshid, E.; Villa, E.; Chipot, C.; Skeel, R. D.; Kale, L.; Schulten, K. *J. Comput. Chem.* **2005**, *26*, 1781.
33. Si-Shen, F.; Li, M.; Win, K. Y.; Guofeng, H. *Curr. Med. Chem.* **2004**, *11*, 413.
34. Wang, Y.; Yu, L.; Han, L.; Sha, X.; Fang, X. *Int. J. Pharm.* **2007**, *337*, 63.
35. Blakeney, B. A.; Tambralli, A.; Anderson, J. M.; Andukuri, A.; Lim, D. J.; Dean, D. R.; Jun, H. W. *Biomaterials* **2011**, *32*, 1583.
36. Li, J.; Mahdi, F.; Du, L.; Datta, S.; Nagle, D. G.; Zhou, Y.-D. *J. Nat. Prod.* **2011**, *74*, 1894.
37. Rubinstein, L. V.; Shoemaker, R. H.; Paull, K. D.; Simon, R. M.; Tosini, S.; Skehan, P.; Scudiero, D. A.; Monks, A.; Boyd, M. R. *J. Natl. Cancer Inst.* **1990**, *82*, 1113.
38. Costache, A. D.; Sheihet, L.; Zaveri, K.; Knight, D. D.; Kohn, J. *Mol. Pharm.* **2009**, *6*, 1620.
39. Gaumet, M.; Vargas, A.; Gurny, R.; Delie, F. *Eur. J. Pharm. Biopharm.* **2008**, *69*, 1.
40. Chernysheva, Y. V. *Mendeleev Commun.* **2003**, *13*, 65.
41. Song, K. C.; Lee, H. S.; Choung, I. Y.; Cho, K. I.; Ahn, Y.; Choi, E. *J. Colloids Surf. A* **2006**, *276*, 162.
42. Sameti, M.; Bohr, G.; Ravi Kumar, M. N. V.; Kneuer, C.; Bakowsky, U.; Nacken, M.; Schmidt, H.; Lehr, C. M. *Int. J. Pharm.* **2003**, *266*, 51.
43. Abdelwahed, W.; Degobert, G.; Stainmesse, S.; Fessi, H. *Adv. Drug. Deliv. Rev.* **2006**, *58*, 1688.
44. Abdelwahed, W.; Degobert, G.; Fessi, H. *Int. J. Pharm.* **2006**, *309*, 178.
45. Cavatur, R. K.; Vemuri, N. M.; Pyne, A.; Chrzan, Z.; Toledo-Velasquez, D.; Suryanarayanan, R. *Pharm. Res.* **2002**, *19*, 894.
46. Yu, L.; Milton, N.; Groleau, E. G.; Mishra, D. S.; Vansickle, R. E. *J. Pharm. Sci.* **1999**, *88*, 196.
47. Abdelwahed, W.; Degobert, G.; Stainmesse, S.; Fessi, H. *Adv. Drug Deliv. Rev.* **2006**, *58*, 1688.
48. Mayhew, S. G. *Eur. J. Biochem.* **1978**, *85*, 535.
49. Gandhi, M.; Srikar, R.; Yarin, A.; Megaridis, C.; Gemeinhart, R. *Mol. Pharm.* **2009**, *6*, 641.
50. Khansari, S.; Duzyer, S.; Sinha-Ray, S.; Hockenberger, A.; Yarin, A. L.; Pourdeyhimi, B. *Mol. Pharm.* **2013**, *10*, 4509.
51. Lim, Y.-B.; Han, S.-O.; Kong, H.-U.; Lee, Y.; Park, J.-S.; Jeong, B.; Kim, S. W. *Pharm. Res.* **2000**, *17*, 811.
52. Price, P. J.; Gregory, E. A. *In vitro* **1982**, *18*, 576.